Conformational Analyses and Molecular-Shape Comparisons of a Series of Indanone–Benzylpiperidine Inhibitors of Acetylcholinesterase

Mario G. Cardozo,[†] Takatoshi Kawai,[‡] Youichi Iimura,[‡] Hachiro Sugimoto,[‡] Yoshiharu Yamanishi,[‡] and A. J. Hopfinger*,[†]

Department of Medicinal Chemistry and Pharmacognosy, M/C 781, University of Illinois at Chicago, P.O. Box 6998, Chicago, Illinois 60680, and Eisai Co., Ltd., Tsukuba Research Laboratories, 1-3, Tokodai 5 chome, Tsukuba, Ibaraki 300-26, Japan. Received June 19, 1991

Conformational analyses and molecular-shape comparisons were carried out on an analogue series of indanone–benzylpiperidine inhibitors of acetylcholinesterase (AChE). It was possible to define an active conformation with respect to the flexible geometry of the benzylpiperidine moiety, as well as an active conformation of the indanone ring–piperidine ring substructure for analogues having a single spacer group between these rings. No active conformation could be postulated for analogues having two or three spacer units between the indanone and piperidine rings. Still, a receptor binding model can be constructed for all indanone and piperidine ring substructures. The postulated active conformation for 1-benzyl-4-[(5,6-dimethoxy-1-oxoindan-2-yl)methyl]piperidine hydrochloride (1a), a potent AChE inhibitor, is close to the crystal structures of 1a with respect to the indanone–piperidine substructure, but differs from the crystal structures for the benzylpiperidine moiety. However, the crystal conformations and the postulated active conformation of the benzylpiperidine portion of the AChE inhibitor are estimated to be about equally stable. A trans-decalin analogue of 1a can adopt the postulated active conformation as shown by calculation and as seen in its crystal structure. The inactivity of this analogue is explained by the added steric size of the decalin unit and/or the time-average valence geometry behavior at the spiro junction to the indanone ring.

Introduction

In the previous paper[1] we described how an extended set of indanone–benzylpiperidines in which **1** encompasses many, but not all, homologues considered in our analyses could be decomposed into four substructural classes with respect to performing both QSAR and molecular modeling analyses. The resulting four individual structure–activity "pictures" could then, in principle, be "viewed", in composite, to afford a global molecular design model.

(1)

(1a); R = 2,3-(OCH₃), R'=H
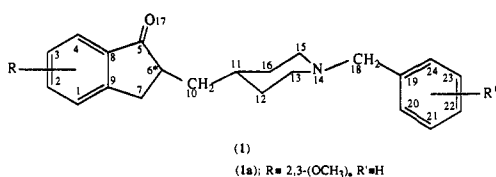
That paper[1] reported the QSAR analyses of feature 1, substitution of the indanone ring, and QSAR analyses of feature 4, substitution of the benzyl piperidine ring. Significant QSARs, involving three-dimensional electronic and spatial descriptors, were constructed and used to make inferences on the nature of AChE binding of the substructures of **1** encompassed within features 1 and 4, see Figure 1 as reference.

This paper discusses the molecular modeling studies of feature 2, conformational and molecular-shape analyses of the combined indanone ring and piperidine ring moiety of **1**, and feature 3, the conformational and molecular shape analyses of the composite piperidine ring and benzyl ring moiety of **1**. The primary objective of these molecular modeling studies is to identify the "active" conformations (molecular shapes) of features 2 and 3. In addition, by concatenating the feature 2 and feature 3 "active" conformations, we hoped to be able to construct an overall active conformation of the backbone structure of **1**.

We have also investigated the molecular shape and conformational features of **1** relative to pseudocongeneric classes of analogues to **1**. The comparative findings of these molecular modeling analyses are also presented
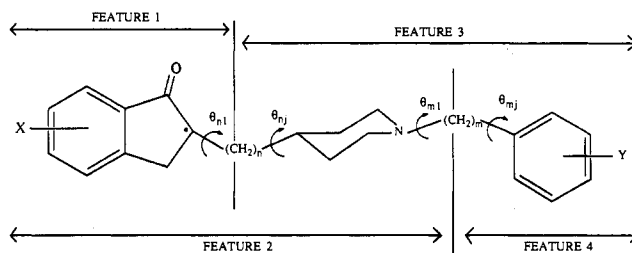

Figure 1. The four features of the indanone–benzylpiperidine AChE inhibitors defined.

within the framework of a generalized spatial molecular shape for AChE inhibition by members belonging to congeneric classes of **1**.

Methods

1. Conformational Analysis. Active conformations were sought by attempting to identify stable intramolecular conformer states for active analogues that are not stable for inactive analogues. We refer to this modeling strategy as applying the LBA–LCS (loss in biological activity–loss in conformational stability) principle.[2]

Conformational stability was estimated by computing the free-space intramolecular conformational energy as a function of the torsion angles. Prior to performing these conformational scans, the valence geometry of each unsubstituted model compound (defined below) was optimized and then held rigid in subsequent conformational scans. All the analogues were constructed using chemical fragments, having standard bond lengths, bond angles, and torsion angles. These fragments are part of the CHEMLAB-II library.[3] A molecular mechanics force field was used which employed an extended and refined version of the MM2 force

---

* Author to whom all correspondence should be sent.
† University of Illinois at Chicago.
‡ Eisai Co., Ltd.

(1) Cardozo, M. G.; Iimura, Y.; Sugimoto, H.; Yamanishi, Y.; Hopfinger, A. J. J. Med. Chem., preceding paper in this issue.
(2) (a) Hopfinger, A. J.; Malhotra, D.; Battershel, R. D.; Ho, A.; Chen, J. Conformational Behavior and Thermodynamic Properties of Phenothrin Analog Insecticide. A. Pest. Sci. 1984, 9, 631–641. (b) Johnson, M. A., Maggiora, G. M., Eds. Concepts and Applications of Molecular Similarity; John Wiley and Sons: New York, 1990.
(3) CHEMLAB-II V11.0. Distributed by Polygen-Molecular Simulations Inc., 200 Fifth Ave., Waltham, MA 02254 (1991).

Table I. The Analogues of, or Similar to, **2** Used To Map the Active Conformation (Shape) of **1** with Respect to Feature **2**

2

no.	A	X	Y	W	IC$_{50}$, nM
			Part A: Active Analogues with Two Torsion Angles (θ_1, θ_2)^a		
1A	-CH$_2$-	CH	N	θ_1 CH$_2$ θ_2 (R)	5.3
1B	-CH$_2$-	CH	N	-CH$_2$- (S)	7.7
2	(indanone =CH$_2$ structure)	CH	N	=CH-	8.4
3	-CH$_2$-	N	N	-CH$_2$-	94.0
			Part B: Inactive Analogues with One, θ_1, or Two Torsion Angles (θ_1, θ_2)		
4	-CH$_2$-	N	CH	-CH$_2$- (R/S)	480.0
5	(indene CH$_3$ structure)	CH	N	-CH$_2$-	4400.0
6	-CH$_2$-	CH	N	-(R/S)	3300.0
7	(indanone CH$_3$ structure)	=C	N	-	1200.0
			Part C: Active Analogues with Three (θ_1, θ_2, θ_3) or Four Torsion Angles (θ_1, θ_2, θ_3, θ_4)		
8	(phthalimide structure)	CH	N	θ_1 CH$_2$ θ_2 CH$_2$ θ_3	0.90
9	(dihydroquinolinedione structure)	CH	N	-(CH$_2$)$_2$-	4.2
10	-CH$_2$-	CH	N	θ_1 CH$_2$ θ_2 CH$_2$ θ_3 CH$_2$ θ_4 (R/S)	1.5
11	(indanone =CH$_2$ structure)	CH	N	=CH(CH$_2$)$_2$-	0.82
12	(indanone =CH$_2$ structure)	CH	N	=CH θ_2 CH=CH θ_4	3.0

^{a} The torsion angle θ_n of the bonded atoms ABCD adopt the value of 0° for the cis-planar arrangement of the bond AB and CD. ^{b} IC$_{50}$ values correspond to analogues of structure **1**.

field[4] as implemented in the MMFF[5] option of CHEMLAB-II.[3] The electrostatic potential was represented by a Coulomb function employing CNDO/2[6] partial atomic charges and an "organic molecular dielectric" of 3.5.[5,7]

All torsion angle scans were first carried out at 30° resolution. The apparent minima identified at this resolution were then used as starting points for complete structure optimization using MMFF in CHEMLAB-II. The *R* and the *S* isomers for the drug candidate, **1a** (R = 2,3-

(OCH$_3$)$_2$, R' = H), with respect to C*, see **1**, were explicitly considered in separate conformational analyses. Only the *R* isomer was considered for all other analogues studied.
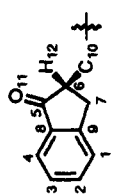
All molecular dynamics (MD) simulations were performed using the MOLSIM package.[8] The force field and electrostatic potentials used were the same as for the molecular mechanics energy minimizations. Prior to each simulation an equilibration process was performed from 20 to 300 K over 3 ps. Subsequently, 10 ps of MD simulation was performed at 300 K.

2. Feature 2. The set of model compounds encompassed in **2** was used to characterize the conformational behavior of the bicycle–piperidine portion of the AChE inhibitor analogues. In **2**, W = (CH$_2$)$_n$ [n = 0, 1, 2, or 3], or a combination of single and double bond spacer units,

(4) Allinger, N. L. Conformational Analyses. 130. MM2. A Hydrocarbon Force Field Utilizing V1 and V2 Torsional Terms. *J. Am. Chem. Soc.* **1977**, *99*, 8127–8134.

(5) Hopfinger, A. J. *Conformational Properties of Macromolecules*; Academic Press: New York, 1973.

(6) Pople, J. A.; Beveridge, D. C. *Approximate Molecular Orbital Theory*; McGraw-Hill: New York, 1970.

(7) Tripathy, S. K.; Hopfinger, A. J.; Taylor, P. L. Theoretical Determination of the Crystalline Packing of Chain Molecules. *J. Phys. Chem.* **1981**, *85*, 1371–1380.

(8) Doherty, D. C. *MOLSIM User Guide*, V2.0. Distributed by The Chem21 Group: 1780 Wilson Drive, Lake Forest, IL 60045; 1990.

Table II. Bicycle Ring Geometries of Compound 1A of Table I

description	torsion angles,[a] deg							
	C8-C9-C7-C6	C9-C7-C6-C10	C9-C7-C6-H12	C8-C5-C6-C7	C9-C7-C6-C5	C3-C2-C1-C6	C3-C2-C1-C7	C5-C8-C9-C7
X-ray A structure	-5.6 (0.4)	-110.9 (0.3)	+125.5	-7.4 (0.3)	7.6 (0.3)	-2.9 (0.3)	-0.9 (0.3)	1.0 (0.4)
X-ray B structure	11.9 (0.3)	-144.1 (0.3)	95.3	18.0 (0.3)	-17.6 (0.3)	3.9 (0.3)	-1.8 (0.4)	-0.7 (0.4)
molecular dynamics of B	14.1	-149.5	96.2	15.3	-16.7	8.9	0.9	-5.3
MOPAC of A	-3.2	-119.1	118.1	-4.7	4.7	-1.9	-0.2	0.1
MOPAC of B	11.5	-141.8	96.6	13.0	-14.5	4.9	-1.1	-3.3
MMFF of B	4.5	-129.7	106.3	5.0	-5.0	1.7	-0.8	-1.5

[a] The values in parentheses correspond to the X-ray root-mean-square deviation in fit.

A, is usually CH_2, but can also be C=O, and X and Y are CH or N.
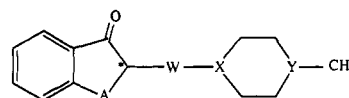
(2)

Table I contains the set of substructure **2** analogues used to investigate feature 2. Each structure in Table I corresponds to an analogue of 1 for which the remainder of the molecule is CH_2Ph and not Me as in **2**. Thus, the variations in IC_{50} reported in Table I are due solely to the structural changes represented by **2**, and the molecular decomposition–recomposition (MDR) technique[1] can be used. Note that a couple of key analogues, with respect to modeling, correspond to changes on the piperidine ring of compound 1: (1) compound **3** in which there is an additional nitrogen atom at position X and (2) compound **4** in which the piperidine nitrogen has been changed from Y to X. Table I is subdivided into part A that contains active inhibitors which have one or two torsion angles (θ_1, θ_2) between the bicycle and the piperidine rings: part B that contains substructure analogues for inactive inhibitors having zero, one, or two torsion angles between the rings; and part C that contains substructure analogues for active inhibitors having three or four torsion angles between the rings. It should be noted that some 6–6 bicycles are contained in Table I. These have been included to provide additional information to map the active molecular shape of feature 2 substructures.

Crystal structures of 1 of Table I have been determined and are discussed below. The crystal structures of the 6–5 bicycle were used as references to evaluate which computational method yields the most reliable bicyclic ring geometry. MMFF,[5] MOPAC (using the MNDO Hamiltonian),[9] and molecular dynamics (MD)[8] were used to determine stable bicycle geometries. The principle concern was the puckering of the five-member ring which can have a very significant influence on the location of the spacer group, W, see Table I, relative to the bicycle. The results are presented in Table II. It appears that only MOPAC predicts a minimum geometry near the crystal B geometry. Thus, the MOPAC B geometry was selected and held rigid in all subsequent static conformational scans. The optimized geometry from MOPAC was used for all other bicyclic ring systems considered in this study.

3. Feature 3. The set of feature 3 derivatives is given in Table III, and the corresponding model compounds used in the conformational analyses can be represented by **3**.
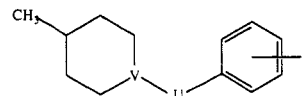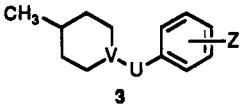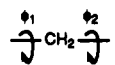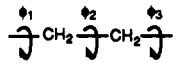

(3)

U is most often CH_2, but can also be C=O and $(CH_2)_2$. The substituted aromatic ring has also been replaced by cyclohexyl and naphthyl rings. Just as in Table I, Table III has also been divided into parts: part A that contains active analogues which have two torsion angles (φ_1, φ_2); part B that contains inactive analogues which have two torsion angles (φ_1, φ_2); and part C that contains a single inactive analogue which has three torsion angles (φ_1, φ_2, φ_3).

All of the analogs in Table III are well-characterized structures having little valence geometry strain. Thus,

(9) Stewart, J. J. P.; Seiler, F. K. QCPE no. 455, V4.0. Indiana University: Bloomington, IN 47405; 1987.

Table III. The Analogues of, or Similar to, **3**, Used to Map the Active Conformation (Shape) of **1** with Respect to Feature 3

| no.	U	V	Z	IC_{50}, nM
Part A: Active Analogues with Two Torsion Angles (ϕ_1, ϕ_2)				
13	ϕ_1 ϕ_2 (–CH₂–)	N	H	5.3
14	$-CH_2-$	N	o-CH_3	10.0
15	$-CH_2-$	N	c-C_6H_{11}	8.9
Part B: Inactive Analogues with Two Torsion Angles (ϕ_1, ϕ_2)				
16	$-CH_2-$	N	o-NO_2	160.0
17	$-C(O)-$	N	H	10000.0
18	$-CH_2-$	N	2-naphthyl	2900.0
19	$-CH_2-$	N	1-naphthyl	220.0
Part C: An Inactive Analogue with Three Torsion Angles (ϕ_1, ϕ_2, ϕ_3)				
20	ϕ_1 ϕ_2 ϕ_3 (–CH₂––CH₂–)	N	H	180.0

[a] IC_{50} values correspond to analogues of structure **1**.

standard bond lengths and angles could be used, and held fixed, in rigid rotation conformational scans of ϕ_1, ϕ_2, ϕ_3. The bond lengths and bond angles of the crystal structures corresponding to **13** of Table III are nearly identical to standard values supporting this modeling simplification.

4. Molecular-Shape Comparisons. Molecular-shape comparisons were performed by first superimposing pairs of molecules under some initial three-atom constraint (spatial pharmacophore) and then using this criterium as a starting point in an optimization of molecular-shape similarity. The measure of molecular-shape similarity has been based upon considering molecular geometry and corresponding conformational energetics. The geometric measures of molecular shape similarity include one, or more, pairs of interatomic distances, and/or, maximizing common overlap steric volume. Conformational energetics have been built into the estimation of molecular-shape similarity by using loss in conformational energy of an analogue (relative to the intramolecular global minimum energy conformation), to achieve an increase in the geometric measure of molecular-shape similarity, as a penalty function to the geometric measure. Upper limits in allowed losses in intramolecular conformational energy have been preset in each molecular-shape comparison.

5. X-ray Crystallography. A single crystal of the drug candidate **1a**, crystallized from methylene chloride solution, was prepared and used. Data collection was performed with Cu Kα radiation (λ = 1.541 84 Å) on an Enraf-Nonius CAD4 computer controlled κ axis diffractometer equipped with a graphite crystal, incident beam monochromator. The crystal was found to be monoclinic, and unit cell parameters were a = 19.364 (6) Å, b = 9.468 (3) Å, c = 11.656 (8) Å, β = 93.04 (5)°, and V = 2134.0 Å³. For Z = 4 and FW = 379.5, the calculated density is 1.18 g/cm³. From the systematic absences of $0k0$, k = $2n$ + 1, and subsequent least-squares refinement, the space group was determined to be $P2_1$. The data were collected to a maximum 2θ of 130.0° using the $2\theta-\omega$ scan technique.

Lorentz and polarization corrections were applied to the data. No absorption correction was made. Intensities of equivalent reflections were averaged. The structure was solved by direct methods. Full-matrix least-squares refinement of atomic positional and thermal parameters (anisotropic C, N, O; isotropic H (fixed at 4.0 Å²)) con-
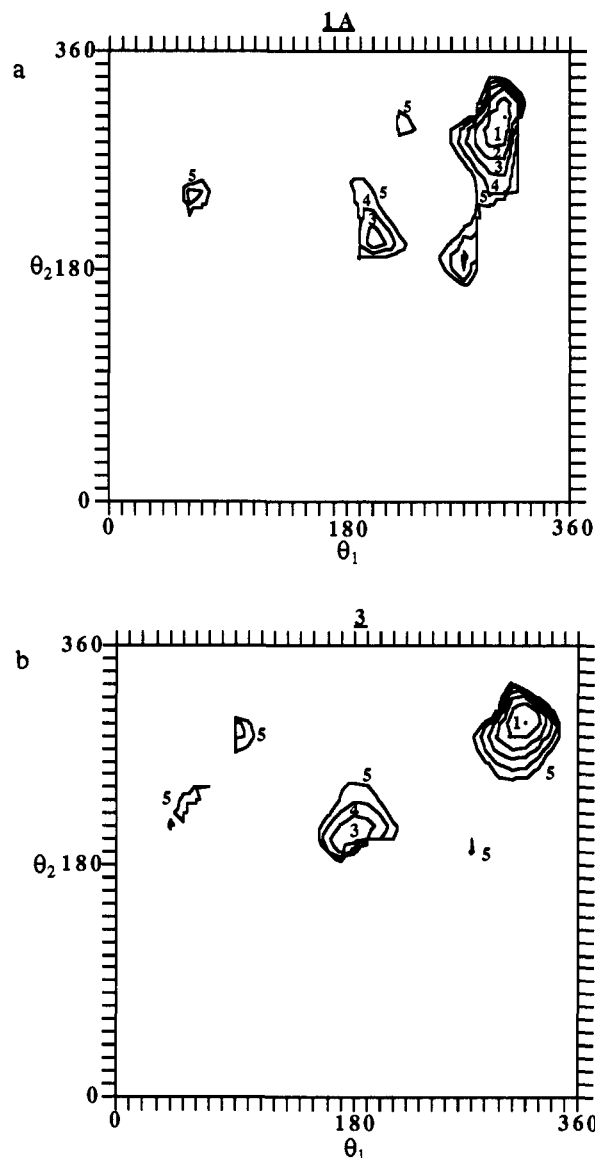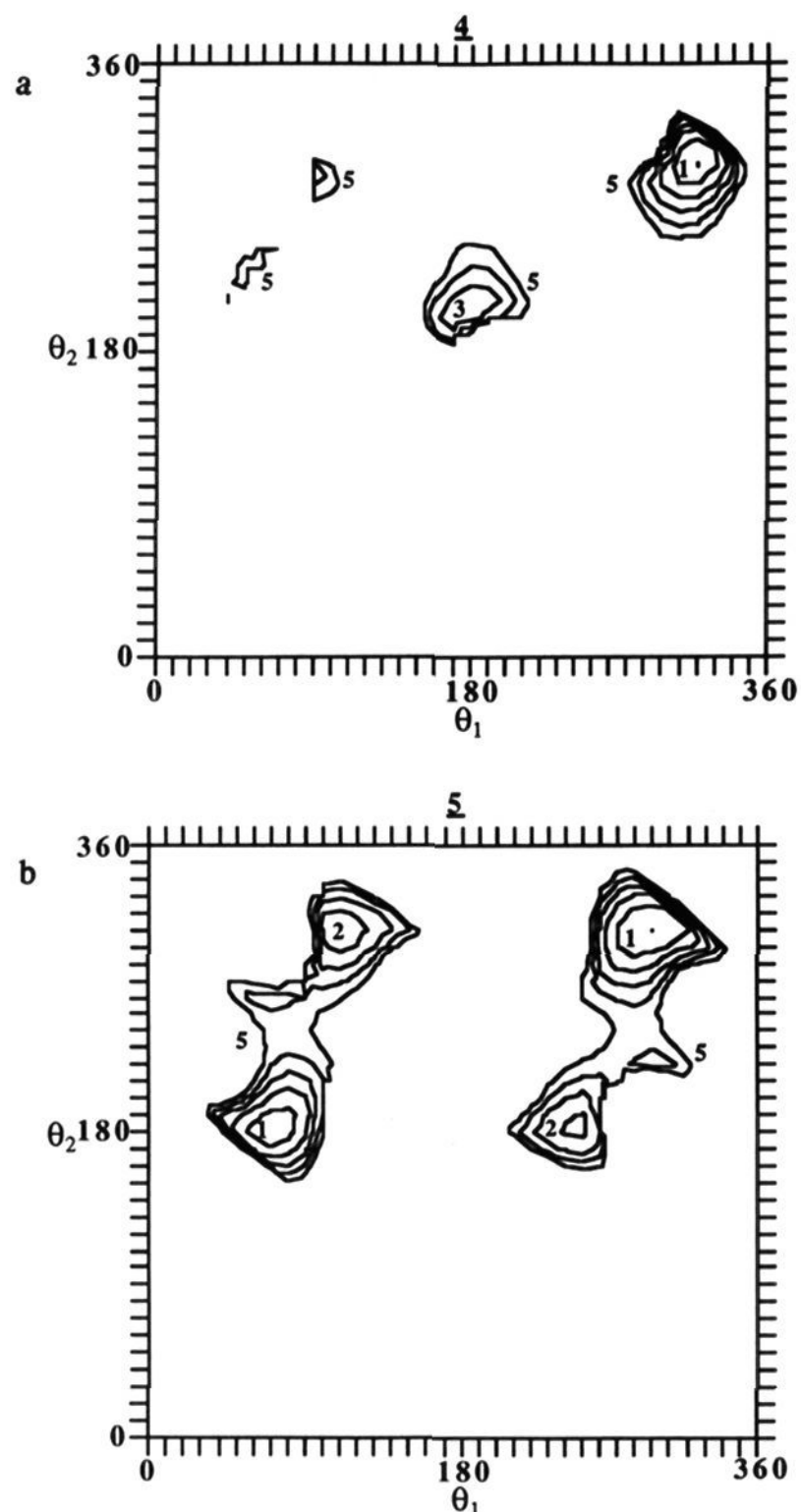

Figure 2. Conformational energy maps of key active analogues of **2** from Table I used to postulate the active conformation (shape) of **1** with respect to (θ_1, θ_2). The energy contours are in kilocalories per mole relative to the global minimum denoted by (●); (a, top) **1A**, (b, bottom) **3**.

verged at R = 0.037 over 3419 reflections with $I > 3\sigma(I)$. All calculations were performed on a VAX11/750 computer using SPD/VAX.

The same procedures used to determine the crystal conformations of **1a** were also employed to solve the crystal structure of the *trans*-decalin analogue **4**. The recrystallization solvent was MEK (methyl ethyl ketone). The unit cell parameters are a = 17.949 (4) Å, b = 5.835 (1) Å, c = 11.309 (4) Å, β = 100.18 (2)°, V = 1165.8 Å³, Z = 2, and D_{calc} = 1.26 g/cm³. The space group is Pc; $2\theta_{max}$ = 150.0°. Thermal parameters were refined anisotropically for C, N, O and isotropically for H (fixed at the same value as B_{eq} of adjacent C or N). The final R value is 0.055 over 2258 reflections with $I > 3\sigma(I)$.

Results

1. Feature 2. The conformational energy maps of structure **1A** and **3** of Table I, with respect to θ_1 and θ_2, are given in Figure 2. The R isomer at C* was arbitrarily chosen for these and all other analogues considered in the conformational analyses. It can be seen that these two

Figure 3. Same as Figure 1, but for the key inactive analogues, (a, top) **4**, (b, bottom) **5**.

active analogues have very similar conformational profiles to one another with three relative minima available to each analogue. The conformational energy maps of two inactive analogues, compounds **4** and **5** of part B of Table I, are presented in Figure 3 and are similar, particularly the conformational profile of **4**, to the (θ_1, θ_2) energy maps of the active analogues. The inactivity of structure **5** can be postulated to be due to the absence of the indanone carbonyl oxygen and/or a change in ring geometry due to the double bond involving C*. This compound has an identical global minimum at $(\theta_1 = 300°, \theta_2 = 300°)$ as compared with the active analogues **1** and **3**. However, the conformational energy maps show a displacement of the local minima near $(\theta_1 = 200°, \theta_2 = 200°)$ for the active analogues to $(\theta_1 = 250°, \theta_2 = 180°)$ for **5**. In order to postulate an active (θ_1, θ_2) conformation, it may be important to stress that **5** does not have a stable conformer near $(\theta_1 = 200°, \theta_2 = 200°)$. However, the molecular-shape similarity/difference between **1** and **5** is not completely specified by comparison of the respective conformational energy maps. It is also important to consider the effect of the change in the hybridization of C* on molecular shape. Figure 4 shows the superposition of compounds **1A** and **5** in their respective global minimum energy states. The superposition criterion
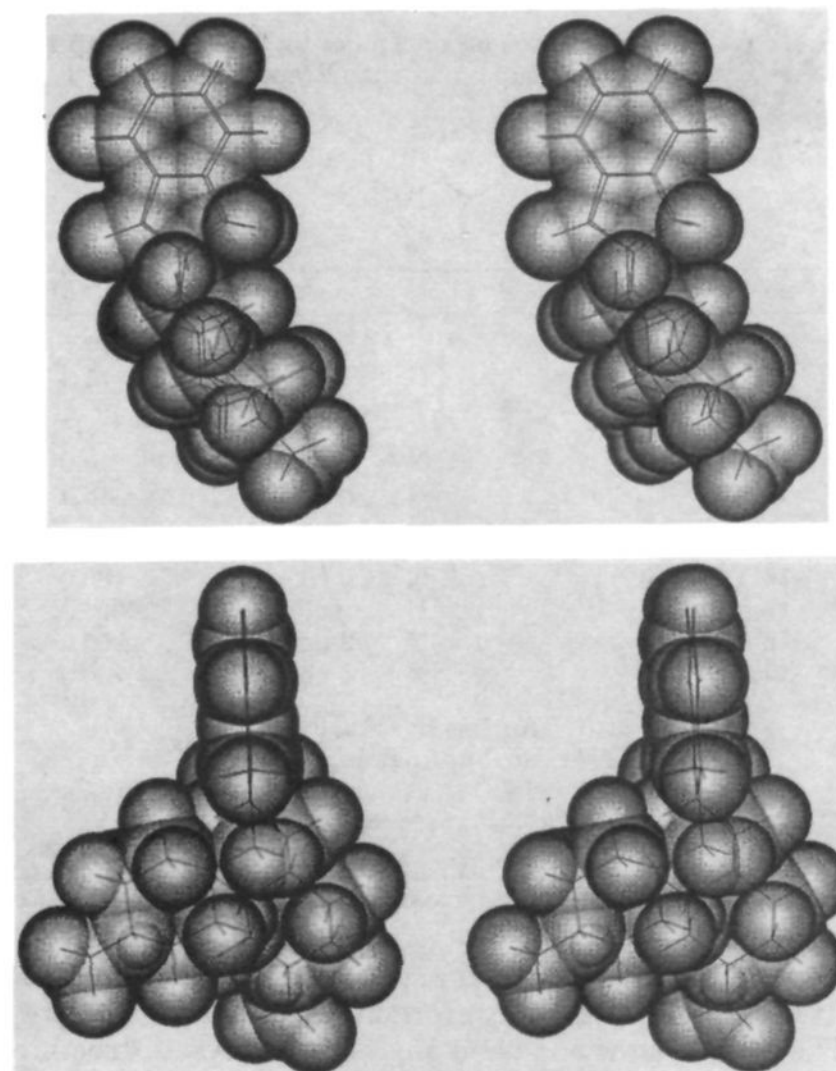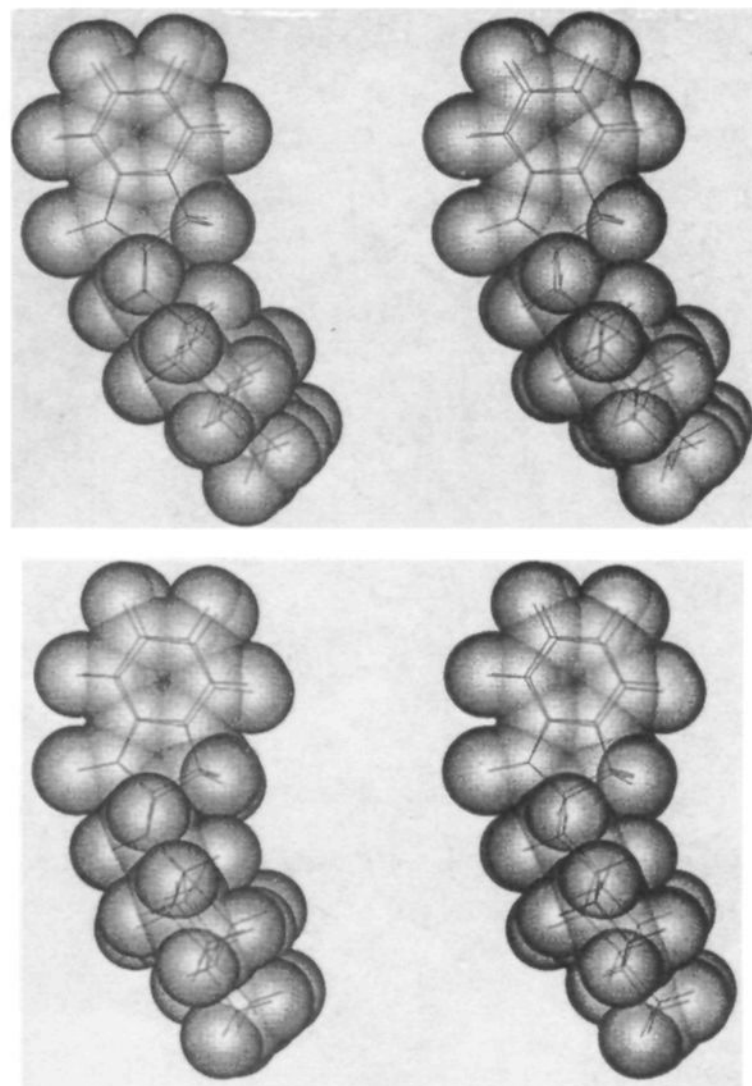

Figure 4. Molecular superposition, shown in stereo, of **1A** and **5** each in their respective intramolecular, global minimum-energy conformation. The superposition criterium is optimum matching of indanone ring geometries. (i, top) View into the plane of the indanone ring. (ii, bottom) View along the plane of the indanone ring.

is the matching of the indanone rings. From Figure 4ii it can be seen that the position of the piperidine ring for compound **5** does not match that of compound **1A** despite the same values of the torsion angles, θ_1 and θ_2. Overall, the molecular shapes defined within feature 2 for the stable intramolecular conformers of compound **5** do not match the molecular shapes of the corresponding minima of compounds **1A** or **3**.

Compound **4** does have the same stable conformers near $(\theta_1 = 200°, \theta_2 = 200°)$, as well as the same global minimum $(\theta_1 = 300°, \theta_2 = 300°)$ as compounds **1A** and **3**. However, all available SAR in these classes of AChE inhibitors suggests the absence of a nitrogen in the 4-position of the piperidine ring is responsible for the loss in inhibition potency of compound **4**.

Overall, the four compounds whose conformational energy maps are shown in Figures 2 and 3 have a common global minimum near $(\theta_1 = 300°, \theta_2 = 300°)$. These compounds also have local minimum energy regions near $(\theta_1 = 200°, \theta_2 = 200°)$, $(\theta_1 = 60°, \theta_2 = 240°)$, and $(\theta_1 = 100°, \theta_2 = 280°)$. At this point, any of the above conformations might be the active conformer. However, it is unlikely that any of the high-energy conformer minima of **1A** and **3** in the upper left-hand portion of their respective energy maps could be the active conformation. Hence, conformations $(\theta_1 = 300°, \theta_2 = 300°)$ and $(\theta_1 = 200°, \theta_2 = 200°)$ are considered the only possible candidates for the active conformation.

Conformational analysis of the trans isomer of compound **2** the other active analogue of Table IA (the cis isomer was found to be a high-energy isomer for all conformer states), indicates two minimum energy states with respect to θ_2. The overall conformational rigidity and very

Figure 5. Molecular superposition, shown in stereo, of 1A in the $(\theta_1 = 300°, \theta_2 = 300°)$ conformation and (A, top) 2 in the $(\theta_2 = 210°)$ conformation, (B, bottom) 2 in the $(\theta_2 = 270°)$ conformation.

Figure 6. Same as Figure 4, but using the $(\theta_1 = 200°, \theta_2 = 200°)$ conformation of 1A.

significant inhibition potency of compound 2 make it a key compound for elucidating the active molecular shape of the analogues in Table IA. Superposition of the conformational minima of 2 with the two possible active conformations of 1A suggests that the conformer $(\theta_1 = 300°, \theta_2 = 300°)$ of 1A is the only one which adopts a similar molecular shape to the minima of 2, see Figure 5. On the other hand, the other possible active conformer $(\theta_1 = 200°, \theta_2 = 200°)$ of 1A differs substantially with respect to the position of the piperidine ring, when compared with both minimum energy conformational states of 2, refer to Figure 6. Therefore, we conclude the $(\theta_1 = 300°, \theta_2 = 300°)$ intramolecular minimum energy state is near the active conformation.

The postulated active conformation for 1A is shown in Figure 7. The observed inhibition potencies of analogues 1B, 3, 6, and 7 of Table I can be interpreted in terms of the molecular shape of 1A in the postulated active conformation. Compound 1B is active and, therefore, must adopt the postulated active conformation, or more correctly, active molecular shape, as a low-energy stable state. Superposition of 1A on 1B in their respective active molecular shapes indicate that these two isomers have their indanone superimposed and that their respective piperidine rings are perpendicular to the bicycle and exhibit partial overlapping. The piperidine nitrogen atoms occupy symmetrical positions with respect to the plane of the indanone ring, and, in this way, both isomers can interact with an active center located at any equidistant position from the piperidine nitrogens. The two isomers differ in molecular shape due to their respective spatial locations of the bridging methylene group.

The inactivity of both 6 and 7 is obviously explained by their being too short, due to the lack of a bridging methylene group, to have their indanone and piperidine rings
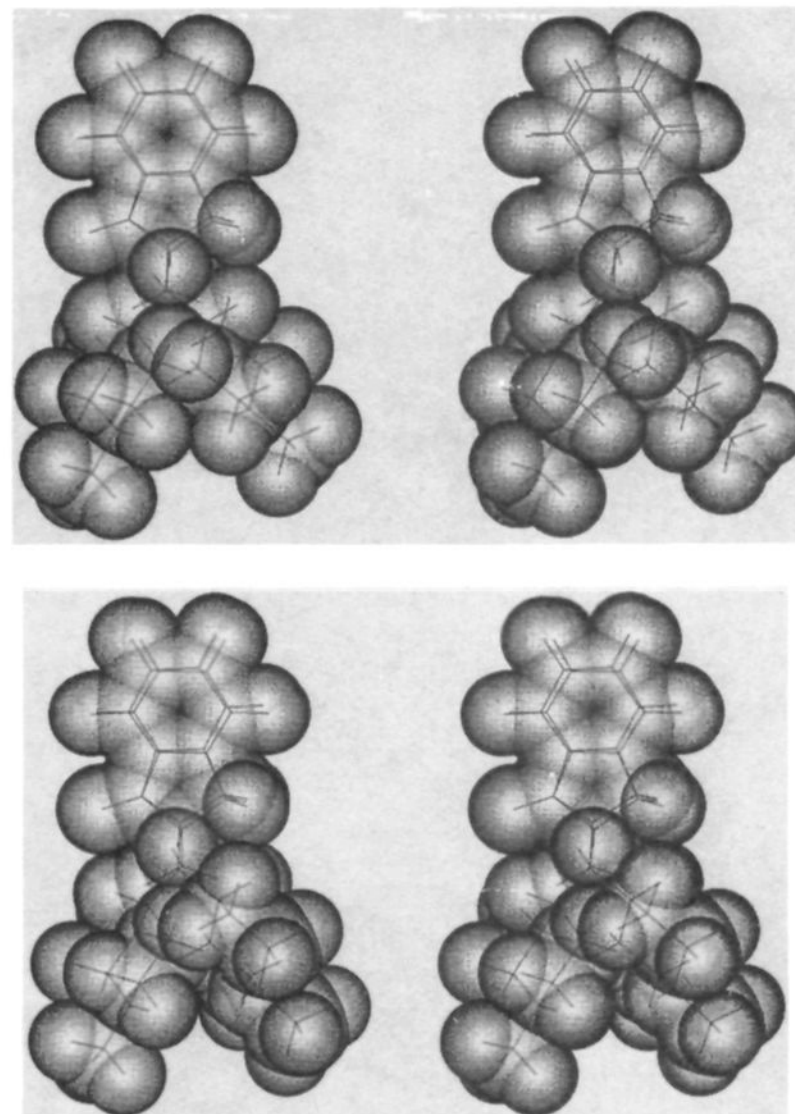
simultaneously superimpose on those of 1A in the active conformation.

Analogue 3 is only 10–15 times less active than the active analogue in Table I, part A. The marginal inhibition activity of 3 is mentioned because it is more difficult to explain the lack of higher activity of this compound than any other analogue in Table I, part A. One possible explanation for the observed activity profile of 3 is based on the active centers hypothesis of the 1 derivatives. The available structure–activity data suggests that both the carbonyl oxygen and the piperidinic nitrogen are essential for AChE inhibition activity. The former is suggested to interact through hydrogen bonding with an acceptor hydroxyl group of a serine residue in the esteratic site of AChE,[10] and the nitrogen is proposed to have a charge–charge interaction with a carboxylic group, possibly an aspartic acid moiety in the anionic site of the enzyme.[10] Therefore, the spatial locations of these "pharmacophoric" atoms are critical for inhibition activity. Spatial considerations are particularly important for the carbonyl group since the hydrogen-bonding interaction is extremely dependent on the distance and the relative orientation geometry of the acceptor and donor groups. Compound 3 has two possible cationic nitrogen centers. Based on the pharmacophore model, the two nitrogens may compete for the anionic center of the enzyme, which is regarded as the orienting site for primary molecular recognition.[11] These competitive interactions may lead 3 to a binding state for which both N atoms are at similar distances from the

(10) O'Brien, R. D. The Design of Anticholinesterases. *Pure Appl. Chem.* 1975, *42*, 1–16.
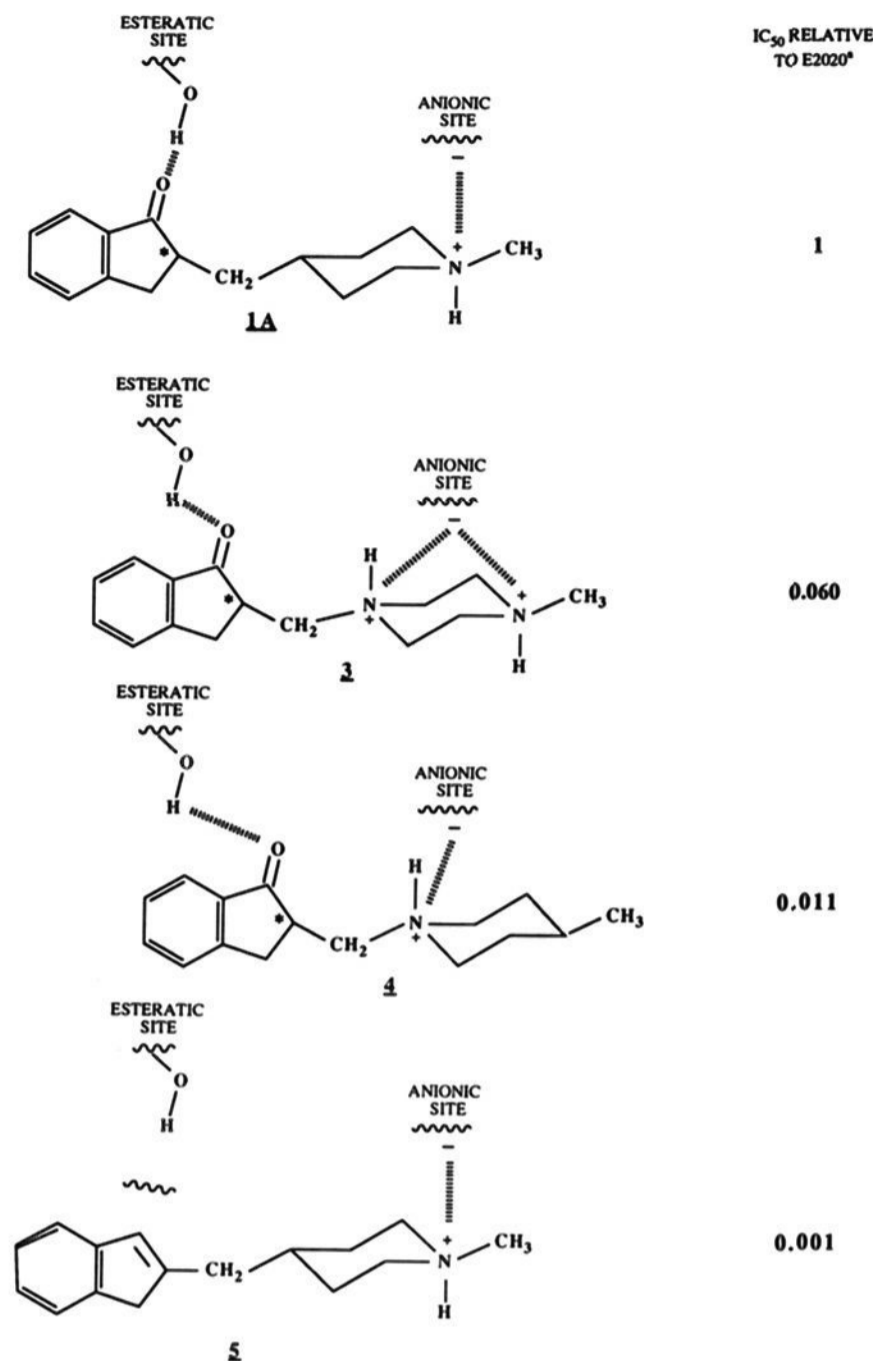
(11) Beckett, A. H.; Al-Badr, A. A. A Modified Structure for the Acetylcholinesterase Receptor. *J. Pharm. Pharmac.* 1975, *27*, 855–858.
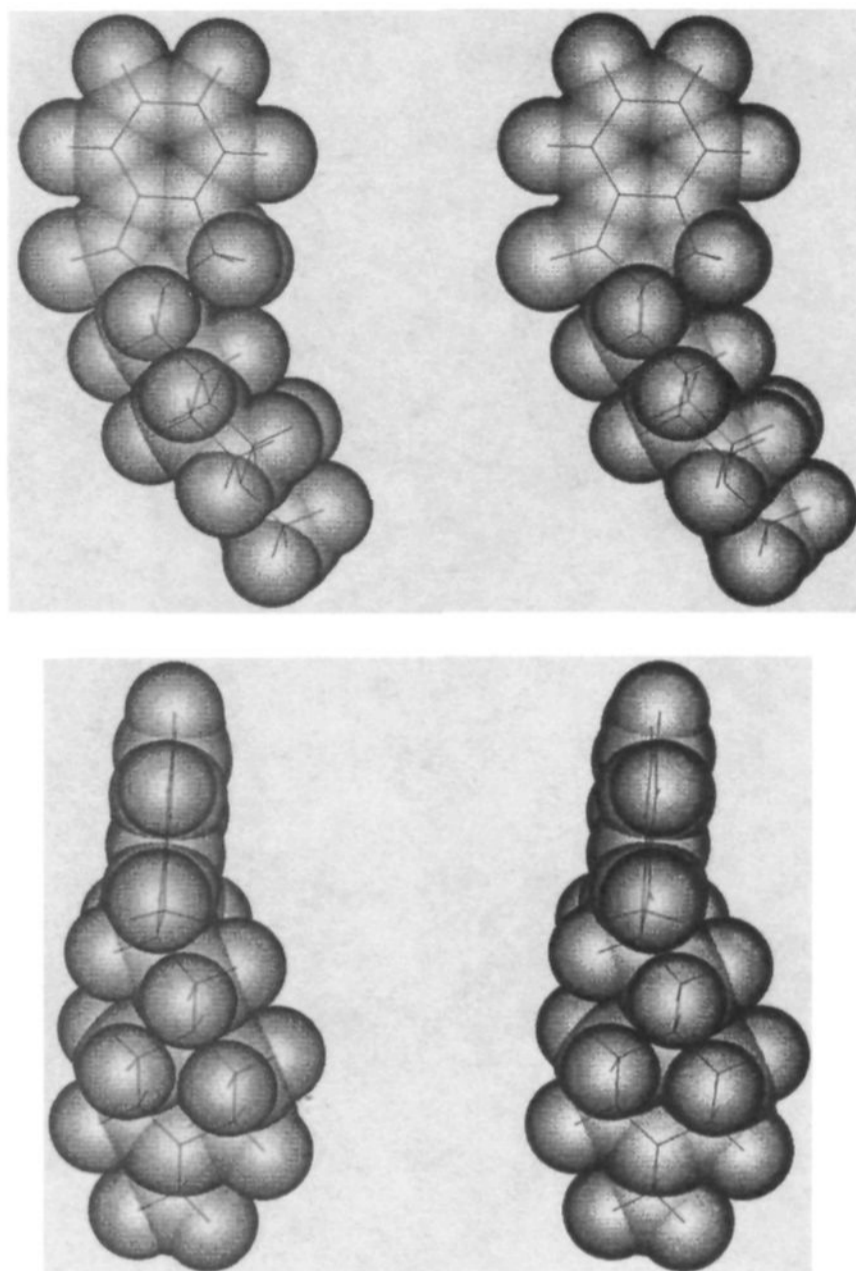
Figure 7. The postulated active conformation for analogues of 2 containing two torsion angles (θ_1, θ_2). The example here is the stereoview of 1A. (i, top) View into the plane of the indanone ring. (ii, bottom) View along the plane of the indanone ring.

Figure 8. Schematic illustration of the esteratic and anionic site interactions for 1A, 3, 4, and 5. The relative activity with respect to 1A is also given. The values reported correspond to dividing the IC_{50} of compound 1A (5.4 nM) by the IC_{50} values of compounds 3, 4, and 5, respectively.

anionic receptor center. Such a virtual "displacement" may move the carbonyl group of the bicycle from its optimum binding position so that the carbonyl oxygen cannot fit properly at the esteratic site. This idea is supported by the biological results reported in Table I for some other analogues. The highly active compound 1A can adopt a position in space near to the optimum interaction geometry. Compound 3, less active than 1A, may have a weak hydrogen-bonding interaction as explained above. Finally, compound 5, the most inactive of the series, can have no hydrogen-bonding interaction, refer to Figure 8. These results also suggest that the hydrogen-bonding interaction is more important than the charge–charge interaction for inhibition of enzyme activity. Compound 4, with both binding centers, but with the carboxylic group located at a shorter distance from the cationic head, is about 100 times less active than 1A. On the other hand, compound 5, with only the cationic head as a possible binding center, is almost 1000 times less active than 1A.

Hypotheses for the "active" conformations (shapes) of analogues of 2 having three or four torsion angles between the indanone and piperidine rings are not as definitive as the model developed for the one and two torsion angle analogues that are described above. There are two reasons for this ambiguity. First, the additional conformational flexibility in the three and four torsion angle analogues makes the exploration of conformational space more difficult. More significant, however, is that inactive three and four torsion angle analogues having structural changes which alter conformational behavior are not available.

Hence, the LBA–LCS principle cannot be used.

An alternate approach to the LBA–LCS principle to probe for active conformation candidates for the analogs in part C of Table I first focused on the conformational analysis of the most rigid analogue in this series, compound 12. The double bonds induce conformational rigidity. All the possible combinations of cis and trans isomers were considered in the conformational analyses of 12. The trans–trans conformational energy minima are generally lower than the minima of the other possible isomers by 3–5 kcal/mol. Thus, we made the assumption that the trans–trans isomer was the relevant bioactive structure. No trans–trans structure adopts a minimum-energy conformation within 5 kcal/mol of its global intramolecular minimum that permits even marginal simultaneous superposition of its indanone and piperidine rings onto those of 1A. Even allowing for conformational distortions up to 5 kcal/mol from each of the relative minima of 12 does not permit any significant superposition fits to the active molecular shape of 1A. It is also not possible to determine any energetically reasonable superpositions of the highly flexible analogues 10 and 11 onto 1A. Compound 10 is the most appropriate analogue to superimpose on 1A since it is highly flexible. However, the superposition of a conformer of 10, which is 2.6 kcal/mol above the global intramolecular energy minimum, indicates that the piperi-
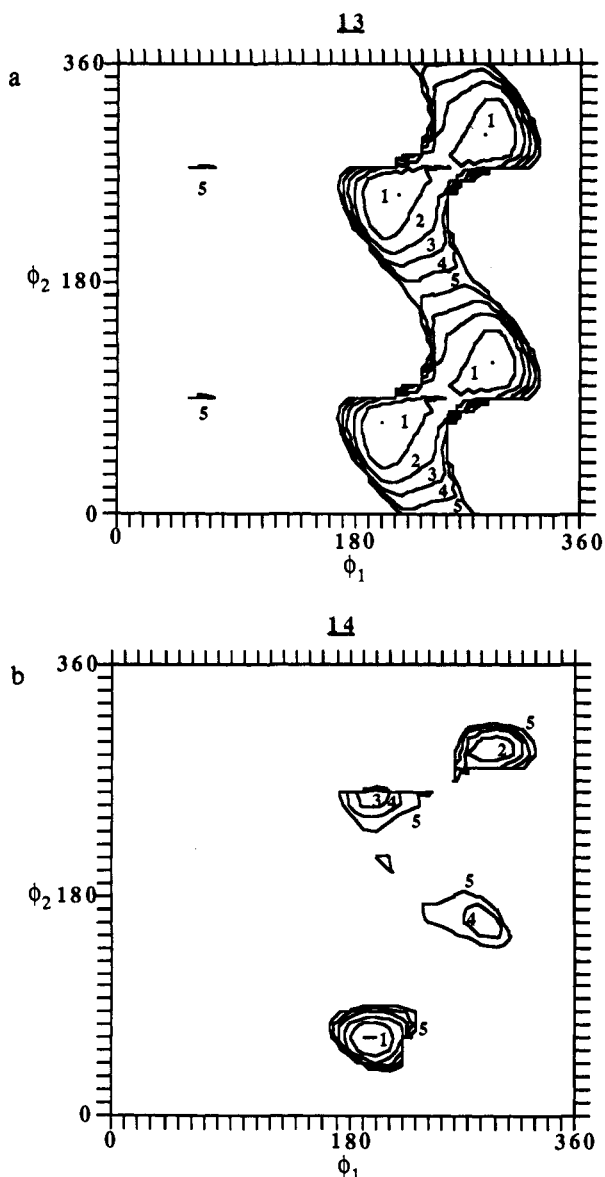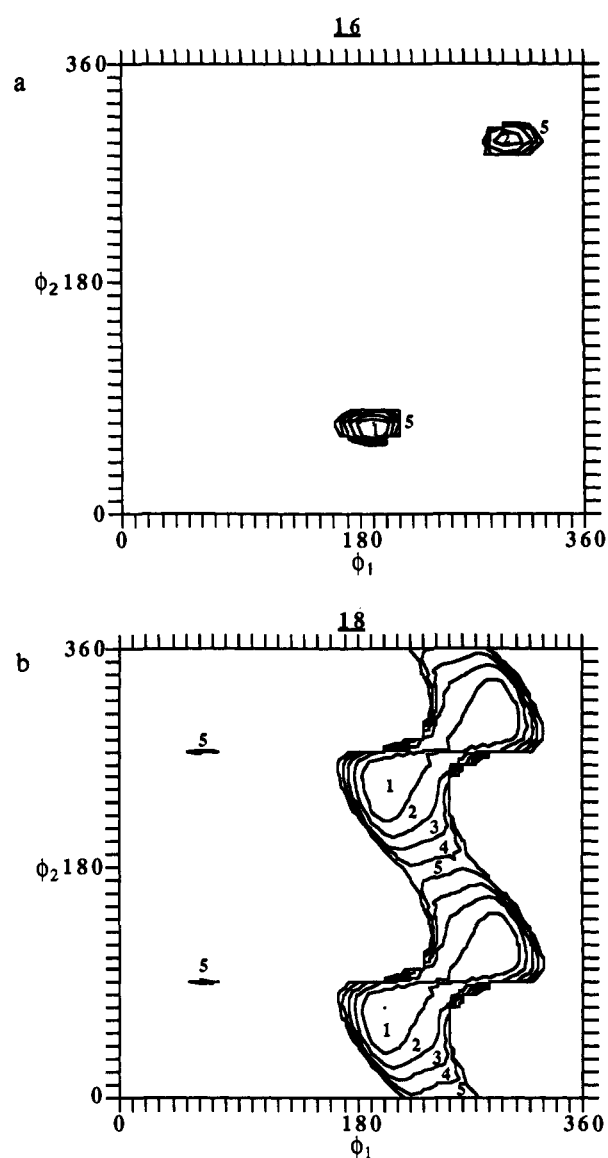
Figure 9. Conformational energy maps of key analogues of 3 from Table III used to postulate the active conformation of 1 with respect to (ϕ_1, ϕ_2). The energy are in kilocalories per mole relative to the global minimum denoted by (●); (a, top) 13, (b, bottom) 14.

Figure 10. Same as Figure 9, but for inactive analogues; (a, top) 16, (b, bottom) 18.

dine rings are quite out register indicating marginal molecular-shape similarity between these two analogues.

The molecular-shape analysis becomes more confusing when stable conformations within 5 kcal/mol of the global minimum of each of the two active analogues having three torsion angles (compounds 8 and 9) are compared to 1A, in its active conformation, and to the stable conformations of 12. In essence, no conformations near the relative minima of 8 or 9 meaningfully superimpose on either 1A or 12. One possible explanation of the differences in molecular shapes among the two, three, and four torsion angle classes of analogues of 2 is that each class has a distinct active molecular shape. This possible explanation of the observed data is further explored later in the paper.

2. Feature 4. The LBA–LCS principle was employed to map out the active conformation of analogues of 3, reported in Table III, with respect to ϕ_1 and ϕ_2. The (ϕ_1, ϕ_2) conformational energy map of the unsubstituted active analogue, 13, is shown in Figure 9A. Figure 9B shows the conformational energy map for the o-CH_3 analogue 14 which is also active. The four minimum energy regions

of 14 overlap with the four minima of 13. However, while 13 has four nearly equal energy minima, 14 has a distinct global energy minimum, two secondary minima, and one high-energy minimum. The high-energy minimum of 14 at (ϕ_1 = 290°, ϕ_2 = 150°) is eliminated as the active conformation because of its high intramolecular conformational energy. The other three conformational energy minima common to 13 and 14 are retained as candidates for the active conformation.

The conformational energy map of the o-NO_2 analogue 16, which is inactive, is shown in Figure 10A. It can be seen that two of the three active conformation candidates of 13 and 14 are also energetically available to 16. These two conformations are thus eliminated using the LBA–LCS principle, leaving the minimum-energy conformation near (ϕ_1 = 200°, ϕ_2 = 240°) as the hypothesized active conformation.

The inactive o,m-naphthyl analogue 19 has a conformational energy map nearly the same as 16, thus accounting for its inactivity. However, the conformational energy map of 18, the inactive m,p-naphthyl analogue is nearly identical to that of 13 (active), compare Figures 10B and 9A. The inactivity of 18 can only be explained by hypothesizing an intermolecular, sterically forbidden, in-
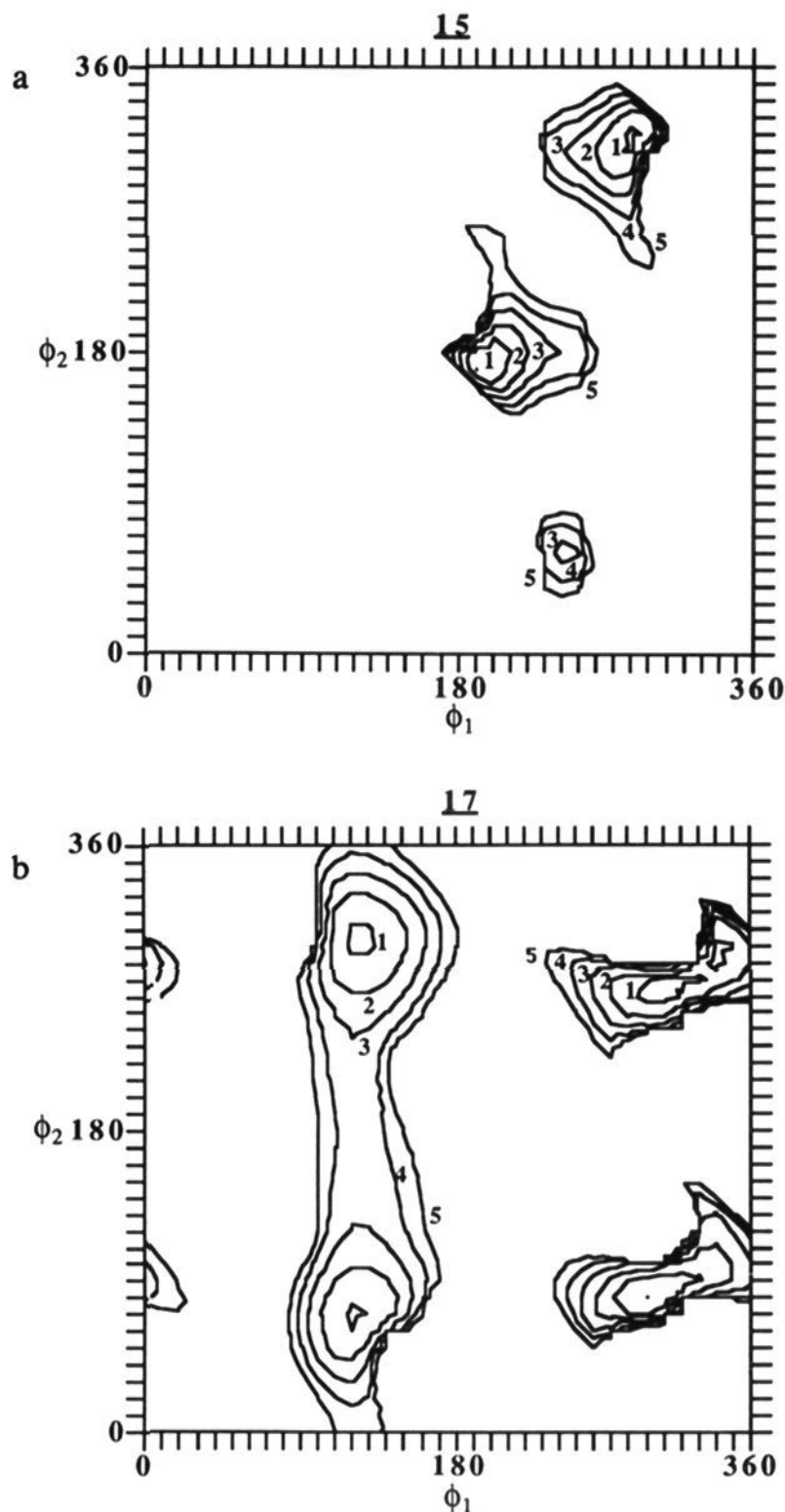
15

17

Figure 11. Same as Figure 9, but for (a, top) **15**, (b, bottom) **17**.

Figure 12. Molecular superposition of **15** and **13** achieved by matching piperidine rings.
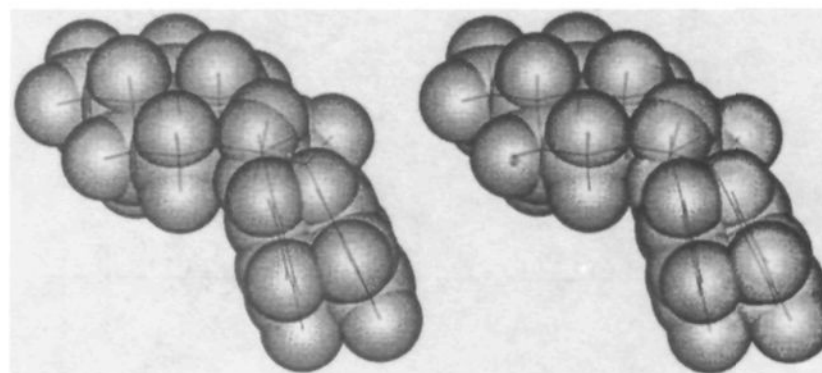
Figure 13. Same as Figure 12, but for **20** and **13**.

teraction between part of the *m,p*-naphthyl ring and the receptor wall. This explanation is consistent with the QSAR developed for substitution onto the phenyl ring in the preceding paper.[1] In particular, Table III of that paper demonstrates a strong inverse relationship between length of the para substituent and AChE inhibition potency. The inactive para methoxy analogue of the data set in Table III of the preceding paper topologically best corresponds to the *m,p*-naphthylene analogue **18**.

The active analogue **15** and the inactive analogue **17** would both be judged to be inactive based upon their (ϕ_1, ϕ_2) energy maps, see Figures 11A and 11B. However, these two energy maps cannot be directly compared to any of the maps in Figures 9 and 10 because **15** and **17** contain valence geometry changes relative to the analogues used to construct Figures 9 and 10. The phenyl ring has been replaced by a cyclohexane ring for **15**. Hence, the geometry of the ring carbon bonded to the methylene spacer (U) is tetrahedral for **15** and not trigonal. Nevertheless, the conformational energy minimum for **15** at ($\phi_1 = 200°$, $\phi_2 = 180°$), see Figure 11A, corresponds to the near perfect superposition of **15** onto **13** in its active conformation. This fit can be seen in Figure 12 where the major difference between **15** and **13**, when superimposed, is the 2,3,4,6 cy-
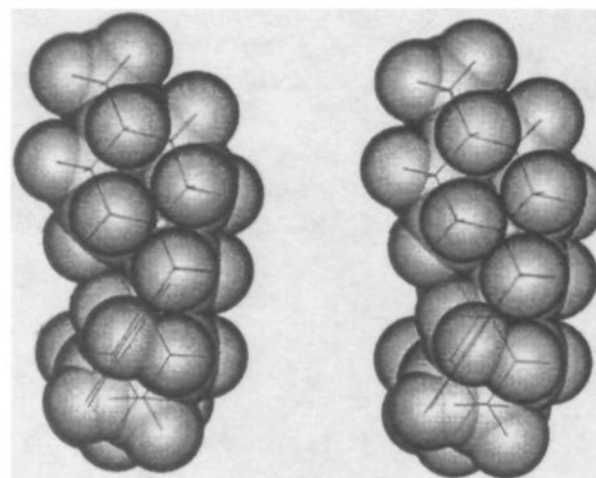
clohexyl CH_2 groups being slightly above and below the plane of the phenyl ring of **13**.

Compound **17** has a carbonyl group, in contrast to a methylene unit, as the spacer between the piperidine and phenyl rings. Thus, the geometry about the spacer carbon is trigonal and not tetrahedral. None of the minima of **17**, see Figure 11B, can be meaningfully superimposed on the proposed active conformation for **13** and **14**. This lack of molecular-shape similarity is assumed to be a source for the inactivity of **17**. In addition, the nitrogen atom of the piperidine ring of **17** has a sp^2 hybridization as part of the amide group. Hence, it cannot protonate, and the compound lacks the cationic head essential for the primary molecular interaction with the enzyme active site.

Finally, the inactivity of **20** of Table III can be accounted for by the fact that it does not possess any energetically reasonable intramolecular conformation which corresponds to a molecular shape that is close to the active molecular shape common to the active analogues—**13**, **14**, or **15**. The optimum molecular superposition of **20** onto **13** is shown in Figure 13. In essence, **20** is too "long" due to the extra methylene spacer.

3. The Active Conformation of 1a: Comparison to X-ray Structures. Application of the LBA–LCS principle during the conformational analyses of analogues of **2** and **3** made it possible to postulate the "active" conformation of **1a** which is shown for the *R* isomer in Figure 14A. The A and B crystal structures of (**1aR**) are shown in Figures 14B and 14C, respectively. Molecular superposition of structures A and B onto the postulated active conformation are shown in Figures 14D and 14E. An inspection of Figures 14D and 14E indicates that both crystal structures adopt conformations very similar to the postulated active conformation with respect to θ_1 and θ_2. However, neither crystal structure adopts the postulated active conformation with respect to ϕ_1 and ϕ_2. The A-form crystal adopts the minimum energy conformation ($\phi_1 = 290°$, $\phi_2 = 300°$) of **13** as shown in Figure 9A. The B form adopts the minimum shown in Figure 9A at ($\phi_1 = 70°$, ϕ_2
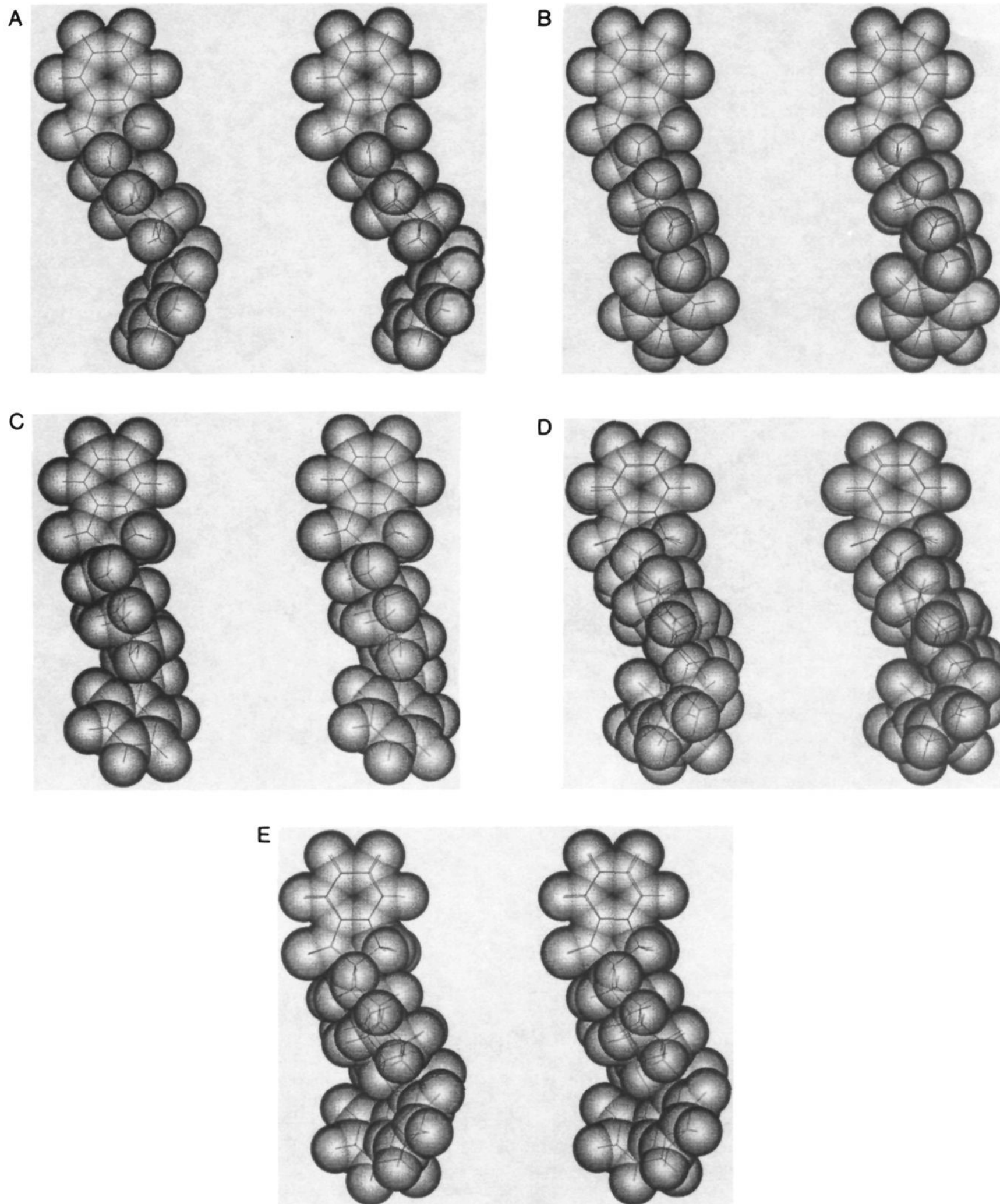
Figure 14. (A) Postulated active conformation of the *R* isomer of **1a**. (B) The A crystal structure of **1a***R*. (C) The B crystal structure of **1a***R*. (D) Molecular superposition of the postulated active conformation of **1a***R* and the A crystal structure of **1a***R*. (E) Same as Figure 14D, but for the B crystal structure of **1a***R*.

= 70°). From an intramolecular energetics standpoint, these two conformations, and that of the active conformation, are all about equally stable, as can be judged from the conformational energy map of Figure 9A. Hence, intermolecular crystal packing forces are likely responsible for the conformational variations in (ϕ_1, ϕ_2) for the A and B crystal conformations of (**1a***R*) from the postulated active conformation.

Discussion

In order to develop an active conformation model for feature 2 analogues having two torsion angles (θ_1, θ_2), it is necessary to postulate that a carbonyl oxygen and a nitrogen that are equivalent, respectively, to the indanone ring carbonyl oxygen, and the 4-N of the piperidine ring are necessary for AChE inhibition potency. If this is not

done, it is not possible to account for the low inhibition potency of analogues 4 and 5 of Table I. However, an implicit consequence of including these two atoms in an active conformation model is the possible atom-pair geometric constraint they represent. The most straightforward geometric constraint is simply the distance between these two atoms which works fine for analogues having two torsion angles—(θ_1, θ_2) analogues. Moreover, there are no stable conformations for the three and four torsion angle analogues leading to a common molecular shape for these two analogue classes which can qualify as a possible second active conformation. Hence, it is either necessary to postulate three distinct active conformations or to construct an active molecular shape binding model consistent with the data of Table I. One possible model is shown in Figure 15. Part A of Figure 15 shows the active analogues in Table I superimposed on one another in such a way that (1) the carbonyl groups are nearly in common, (2) the nitrogens lie approximately in a plane which contains the inandone ring, (3) the nitrogens are all approximately the same distance from a common (receptor) point R, (4) each of the conformations shown in Figure 15A is within 2 kcal/mol of the respective global intramolecular minimum-energy conformation.

Figure 15B shows the inactive analogues of Table I superimposed so that their carbonyl groups are nearly in common. The conformations shown are intramolecular energy minima, within 5 kcal/mol of each respective global minimum, which maximize their respective overlap steric volumes with that of 1A of Table I. None of the inactive analogues have three or four torsion angles between rings. Thus, 1A was considered the most appropriate conformation/molecular-shape comparison reference compound. It is quite obvious from a comparison of Figures 15A and 15B that the inactive analogues are quite different in conformation and shape from the active analogues. The active analogues cluster their net molecular volumes near the plane of the inandone ring while the inactive analogues are markedly skewed from this plane.

The common active shape–pharmacophore hypothesis described above and displayed in Figure 15A, is speculative in that the available structure–activity data is insufficient to rigorously define and/or test the model. In particular, there are no highly inactive three and/or four torsion angle analogues available to define the intramolecular conformational requirements for activity using the LBA–LCS principle.

The proposed active conformation for (θ_1, θ_2) feature 2 analogues is characterized by the indanone and piperidine rings being "perpendicular" to one another. In this description the larger of the two thickness dimensions of the piperidine ring contains its plane relative to the indanone ring. A rigid analogue consistent with this postulated active conformation and molecular shape is the *trans*-decalin analogue shown in **4**.


(4)
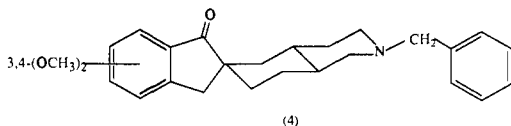
The superposition of the crystal structure of **4** on **1aR** in its postulated active conformation is shown in Figure 16A. These two analogues are seen to be very similar in overall steric molecular shape. The corresponding superposition compound **4** (after MOPAC (MNDO) full optimization on the X-ray crystal structure), on compound **1A**, is shown in Figure 16B. The two conformations are very close in atomic geometry, suggesting the crystal structure
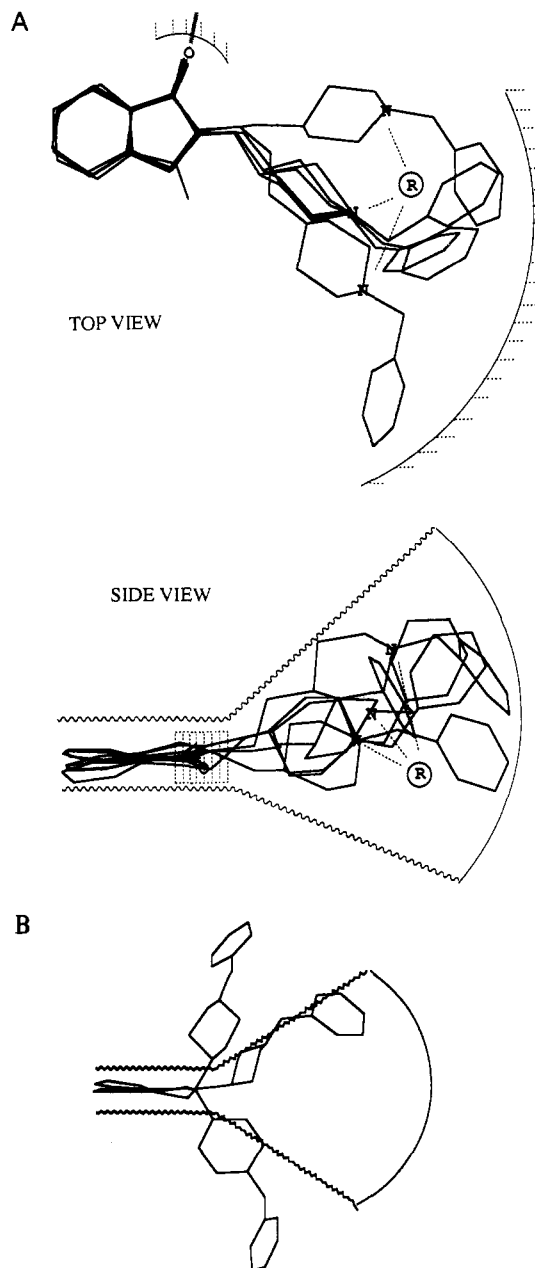
Figure 15. (A) Molecular superposition of the active analogues in Table I under the criterium of maximizing overlap steric volume of each analogue with (**1aR**) in its active conformation. R is a postulated anionic receptor site, which is estimated to be 6.7 ± 0.2 Å from each of the nitrogens of the compounds. (B) Same as Figure 15A, but for the inactive analogues of Table I.

is also an intramolecular energy minimum.

Analogue **4** is quite *inactive* as a AChE inhibitor having an IC_{50} of 2530 nM. The inactivity of **4** obviously is a surprise given the high molecular shape similarity between it and **1A**. We have sought possible reasons for the poor inhibition potency of **4**. One steric molecular-shape difference between **4** and **1A** can be observed in Figure 16A. Two of the methylenes of the cyclohexyl ring of the 6–6 bicycle of **4** occupy a space not encompassed by **1A**. Further, this space is occupied by the minimum-energy conformations of some highly inactive analogues, compare, for example, **7** in Figure 15B to the *trans*-decalin analogue **4** in Figure 16A. This line of reasoning suggests that at least part of the space occupied by the two cyclohexyl methylenes, not in common with **1A** for the postulated $(\theta_1,$
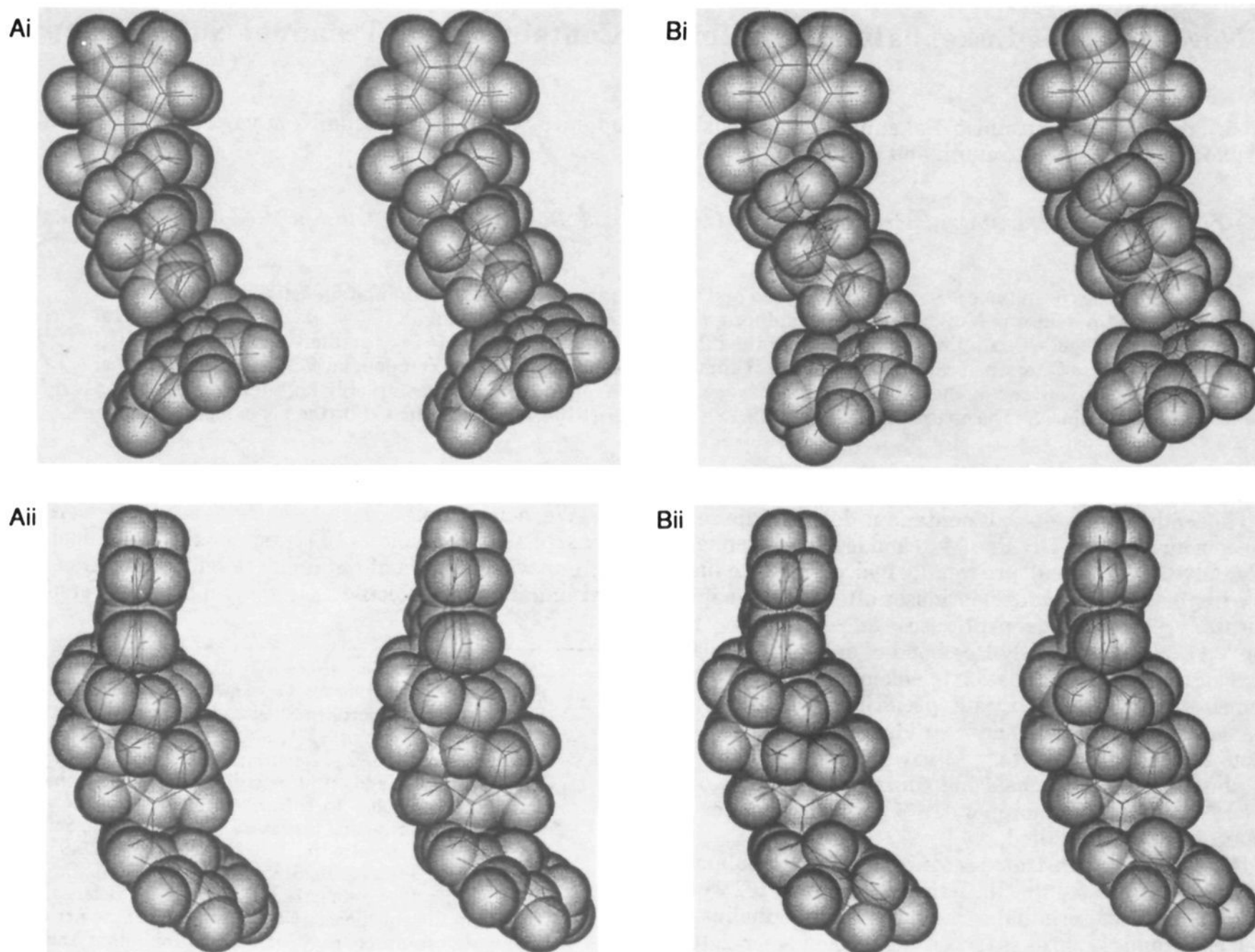
Figure 16. (A) Molecular superposition of **1A**, in its active conformation, and the *trans*-decalin analogue **4**, in its crystal conformation. (i) View into the plane of the indanone ring. (ii) View along the plane of the indanone ring. (B) Same as Figure 16A, but using the MOPAC-optimized geometry of **4**.

Table IV. Molecular Dynamics, Average Location, and Standard Deviation for Atoms 6 and 10; See 1, of Compounds **1A**, **2**, and **4**

analogue	atom no.	$\langle X \rangle$	ΔX	$\langle Y \rangle$	ΔY	$\langle Z \rangle$	ΔZ
1A	6	0.108	±0.208	−1.262	±0.054	2.037	±0.060
1A	10	−0.870	±0.362	−2.354	±0.164	1.624	±0.170
2	6	−0.014	±0.158	−1.060	±0.059	2.052	±0.076
2	10	−0.038	±0.327	−2.319	±0.061	1.316	±0.161
4	6	0.009	±0.252	−1.267	±0.061	2.043	±0.074
4	10	−1.204	±0.379	−2.113	±0.232	1.700	±0.200

θ_2) active conformation, violates receptor space leading to a steric repulsion and loss in inhibition potency.

Another model to explain the inactivity of **4**, which is partially complementary to the steric model described above, involves the molecular freedom about C_6 (C*) of the inandone ring. One would expect **4** to be more rigid than the nonspiro analogues with respect to valence geometry distortions about C_6. Thus, the role of molecular flexibility at C_6 as a possible activity correlate merited exploration. Molecular dynamics (MD) calculations were performed on **1A**, **2** (Table I), and **4** using the MD package MOLSIM. The minimum energy conformation of each compound found from MOPAC was used as an MD starting point. The results are presented in Table IV where it is seen that **1A** has a different time-average puckering about C_6 as compared to **4** and **2**. Analogue **1A** has the C* atom at an average

position out of the plane of the five-membered ring. The other two compounds exhibit time-average positions in the plane of the five-membered ring. This difference in puckering brings the atom bonded to the bicycle, atom 10 of **1A**, to a position closer to the plane of the indanone ring as compared to compound **4**. Therefore, the puckering about C* for **1A** actually leads to minimizing, over time, the difference in the molecular-shape component due to its bridging methylene unit when compared to the dynamic behavior of **2**.

Overall, we are able to postulate a distinct active molecular shape for analogues having two torsion angles (θ_1, θ_2) between the indanone and piperidine rings. A nonunique three-dimensional pharmacophore can be suggested for all of the analogues investigated. Crystal structures of some of the analogues are in the hypothesized active conformation with respect to θ_1, and θ_2, but not with respect to ϕ_1 and ϕ_2. However, the crystal structure (ϕ_1, ϕ_2) conformations are local intramolecular minimum energy states.